A numerical investigation on the flow physics of koi carp (*Cyprinus carpio koi*) burst-and-coast swimming

Yan Yang [a,*] Guan-hao Wu [b], Yong-liang Yu [c] and Bing-gang Tong [c]

[a] Institute of Mechanics, Chinese Academy of Sciences, Beijing 100190, China
[b] State Key Laboratory of Precision Measurement Technology and Instruments, Department of Precision Instruments, Tsinghua University, Beijing 100084, China
[c] The Laboratory for Biomechanics of Animal Locomotion, Graduate University of Chinese Academy of Sciences, Beijing 100049, China

Abstract—Burst-and-coast is the most common locomotion type in freely routine swimming of koi carps (*Cyprinus carpio koi*), which consists of a burst phase and a coast phase in each cycle and mostly leads to a straight-line trajectory. Combining with the tracking experiment, the flow physics of koi carp's burst-and-coast swimming is investigated using a novel integrated CFD method solving the body-fluid interaction problem. The dynamical equations of a deforming body are formulated. Following that, the loose-coupled equations of the body dynamics and the fluid dynamics are numerically solved with the integrated method. The two burst modes, MT (Multiple Tail-beat) and HT (Half Tail-beat), which have been reported by the experiments, are investigated by numerical simulations in this paper. The body kinematics is predicted and the flow physics is visualized, which are in good agreement with the corresponding experiments. Furthermore, the optimization on the energy cost and several critical control mechanisms in burst-and-coast swimming of koi carps are explored, by varying the parameters in its self-propelled swimming. In this paper, energetics is measured by the two mechanical quantities, total output power C_P and Froude efficiency Fr. Results and discussion show that from the standpoint of mechanical energy, burst-and-coast swimming does not actually save energy comparing with steady swimming at the same average speed, in that frequently changing of speed leads to decrease of efficiency.

Index Terms—burst-and-coast swimming, CFD (computational fluid dynamics), fluid-body interaction, self-propelled swimming, *Cyprinus carpio koi*

I. INSTRUCTIONS

Burst-and-coast (also called kick-and-glide) swimming is commonly used by some species of freshwater fish [1, 2]. Its kinematic characteristics has been well known, that each periodic behavior consists of two distinct stages, one stage includes one or more BCF (body and/or caudal fin) locomotory cycles (named burst stage) and the other subsequent unpowered stage (named coast stage). Burst-and-coast swimming happens very frequently in koi carp (*Cyprinus carpio koi*) routine swimming, i.e. spontaneous swimming behavior [3]. Most of previous experimental studies on burst-and-coast swimming focused on the flow pattern and the issue whether the locomotion of burst-and-coast has energetic advantage, as reviewed by Wu et al. [3].

Most of the experimental works, based on certain theoretical models and kinematic data, suggest that burst-and-coast swimming saves more energy than steady swimming at the same average speed, where the steady flow assumption and approximate evaluation of energy cost must be enforced. Weihs [4] firstly developed a theoretical model to estimate the energetics and showed that fish can swim more efficiently by alternating periods of the burst and coast motion. Succeeding works [1, 2, 5] analyzed more experimental data and gave more conditions and examples on obtaining energetic advantages of burst-and-coast swimming, based on the theoretical model of Weihs [4]. Wu et al. [3] studied koi carp's burst-and-coast swimming kinematics, hydrodynamics and energetic advantages, based on a tracking measurement system. Almost all of above experimental and theoretical works are based on the assumption that the hydrodynamics is steady and the drag ratio α (ratio between hydrodynamic drag of active swimming and that of gliding) is a constant (e.g. α = 3, referenced in [2]), which are quite inaccurate in burst-and-coast swimming. In fact, hydrodynamics of burst swimming is typically unsteady, where kinematic data could not afford enough information on flow physics, therefore more accurate model is needed to understand the flow physics of burst-and-coast swimming.

Since unsteady hydrodynamics must be computed, CFD (computational fluid dynamics) should be the most promising tool. In addition, fluid-body interaction should be considered, as a part of the mechanical chain of fish locomotion. That is to say, the fish should be simulated as an active self-propelled body in the flow

* Corresponding author: No. 15, Beisihuanxi Rd., Institute of Mechanics, CAS, Beijing 100190, China P.R., E-mail: yangy@ustc.edu

[6-10], which is more realistic, comparing to the model of a tethered body [11, 12]. To the authors' knowledge, among existing works, almost no simulation-based case of free and self-propelled maneuvering fish has been investigated based on the full Navier-Stokes equations, as follows. Liu et al. [11] firstly implemented the CFD method to study flow physics in tadpole swimming. Borazjani and Sotiropoulos [12] investigated the effect of *Re* number and *St* number in the tethered steady carangiform swimming. Carling et al. [6] firstly proposed the concept of "self-propelled" in CFD simulation of fish swimming, though the body dynamical equation in the work holds only in a discrete system. Kern and Koumoutsakos [8] proposed a better algorithm of body dynamics, while only two kinds of steady anguilliform swimming were investigated.

We have built a CFD platform to simulate a self-propelled freely swimming body [7, 10], which is more realistic to study the hydrodynamics of a maneuvering fish. On the platform, built upon the dynamical equations of deforming body, fluid-body interaction induced by the actively deforming body can be simulated properly. The flow physics of burst-and-coast swimming of koi carp (*Cyprinus carpio koi*) was investigated in this paper. At first, we simulated two basic paradigms of burst-and-coast of koi carp according to the body deforming kinematics from the original experiments, and then the characteristics of the flow physics and some critical control mechanisms are investigated. The energetics was estimated, to evaluate whether and under what condition, burst-and-coast swimming is more advantageous than steady swimming.

II. METHODS

A. Tracking measurement and the undulating kinematics

The measurements were carried out on koi carps (*Cyprinus carpio koi*) by using a video tracking system developed by Wu et al. [3]. The system was used for simultaneous measurements of kinematics and flow of koi carps with burst-and-coast swimming.

The measurements afford the whole kinematics, i.e. the undulating kinematics and the whole-body kinematics, which are the known and the unknown respectively in the simulation (see the next section). As for the undulating kinematics, the tracking measurements of koi carps burst-and-coast swimming [3] suggested that there are two basic burst modes in burst-and-coast swimming, where MT (Multiple Tail-beat) burst includes one tail-beat cycle or more and HT (Half Tail-beat) burst includes only a half tail-beat. The typical samples of both modes of the same koi carp are selected to be investigated by simulating, corresponding to the selected two bouts in [3].

Firstly, by processing with the original experimental images, the mid-line curves history is obtained (Fig. 1). Secondly, the data were fitted with the proposed function used to describe the undulating kinematics. The function is written as below, similar to that in the literature [1],

$$d = A_{\max} a_1(X) a_2(t) \sin\left[2\pi\left(\frac{t}{T} - \frac{X}{\lambda}\right) + \varphi_0\right] + d_0(X) \quad (1)$$

Details of above equation were explained in [10]. The two modeled mid-lines are shown in Fig. 2, which are close to the experimental ones (Fig. 1) and convenient to be used for the simulation because of its good mathematical properties, such as smoothness and continuity. The distinct characteristics of undulating movement between the two burst modes are displayed: (1) the MT burst (A in Fig. 1 and Fig. 2) includes one complete tail-beat cycle which consists of two stage, burst 1 ($0 < t/T < 0.75$) to the right and burst 2 ($0.75 < t/T < 1.5$) to the left; (2) the HT burst (B in Fig. 1 and Fig. 2) includes only a half tail-beat cycle (a burst to the right), therefore it can be divided into two stages, up stroke ($0 < t/T < 0.3$), where the tail swings from its straight position to the one maximum offset and down stroke ($0.3 < t/T < 0.75$), the tail back to straight.

The body length of the koi carp, i.e. the characteristic length is $L^* = L = 0.0556$ m, and a two-dimensional NACA0012 foil is used to simulate its body.

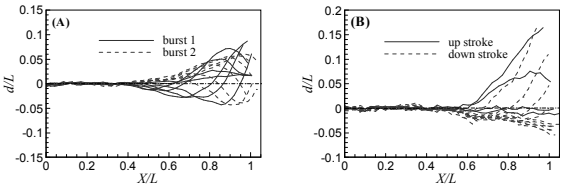

Fig. 1 Mid-line undulating kinematics of koi carp burst-and-coast swimming from the experimental data, plotting with respect to the rigid head. (A) MT mode, (B) HT mode.

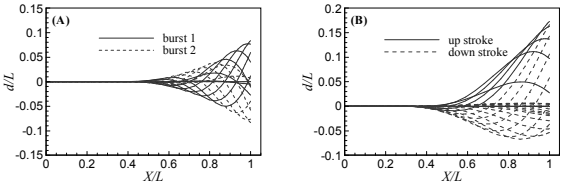

Fig. 2 Mid-line undulating kinematics of koi carp burst-and-coast swimming for simulation. (A) MT case, $T^* = T = 0.16$ s, $A_{\max} = 0.085$ L, $\lambda = 0.57$ L, $X_0 = 0.4$ L; (B) HT case, $T^* = T = 0.32$ s, $A_{\max} = 0.175$ L, $\lambda = 1.386$ L, $X_0 = 0.3$ L.

B. Deforming body dynamics

For body-fluid interaction, the coupled problem of deformable body dynamics (BD) and unsteady fluid dynamics (FD) was solved by the integrated method, on the in-house CFD platform [7, 10]. The process of the simulation is as below: given the undulating kinematics from the experiments, the flow field and fluid forces are calculated, following that the whole-body kinematics is predicted, based on FD and BD.

The critical step to derive the dynamical equations of a deforming body is to introduce the centre-of-mass (c.m.) frame (*Cx'y'* in Fig. 3). The translation and rotaion of this frame, are regarded as the whole-body motion of the fish body, which are determined by the external forces, including the resultant force $\boldsymbol{F}^{(e)}(t)$ and the moment $\boldsymbol{M}_C^{(e)}(t)$. The deforming motion with respect to *Cx'y'* (namely undulating kinematics) is

determined by the internal forces. The above two motions compose the complete motion, both of which are independent with each other. Thus, the governing equations of deforming body dynamics are presented as two parts. The first part consists of the theorems of linear and angular momentum of the deforming body for the whole-body motion:

$$\frac{d}{dt}\left[m\boldsymbol{u}_C(t)\right] = \boldsymbol{F}^{(e)}(t) \tag{2a}$$

$$\frac{d}{dt}\left[I_C(t)\boldsymbol{\omega}_C(t)\right] = \boldsymbol{M}_C^{(e)}(t) \tag{2b}$$

The second part consists of the conservation laws of linear and angular momentum for the deforming motion:

$$\frac{d}{dt}\int \boldsymbol{u}'(s,t)\rho(s)w(s)ds = 0 \tag{3a}$$

$$\frac{d}{dt}\int \boldsymbol{r}'(s,t)\times\boldsymbol{u}'(s,t)\rho(s)w(s)ds = 0 \tag{3b}$$

Equations (3a, 3b) are used to determine $\boldsymbol{u}'(s,t)$ and the transformation between the c.m. frame and the experimental body-fixed frame.

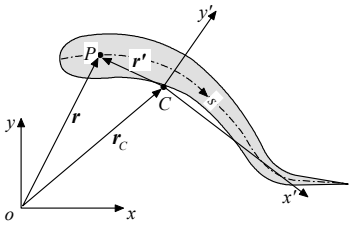

Fig. 3 Inertial coordinate system *Oxy*, and the c.m. coordinate system *Cx'y'*, of the sketched fish model

C. Fluid dynamics: Navier-Stokes equations and the integrated methods

The external action on the fish body, as well as the time-changing fluid force, is got by solving the two-dimensional incompressible, unsteady Navier-Stokes (N-S) equations, with a pseudo-compressible approach. Write the governing equations, in the non-inertial frame *Cx'y'*, which has a translational acceleration $\boldsymbol{a}$ and an angular velocity $\boldsymbol{\Omega}$ (namely $\boldsymbol{\omega}_C$):

$$\begin{aligned}&\int_{V(t)} \mathbf{f}dV + \int_{V(t)} \left(\frac{\partial \mathbf{Q}}{\partial t} + \frac{\partial \mathbf{q}}{\partial \tau}\right)dV \\ &+ \int_{V(t)} \left(\frac{\partial \mathbf{F}}{\partial x} + \frac{\partial \mathbf{G}}{\partial y} + \frac{\partial \mathbf{F}_v}{\partial x} + \frac{\partial \mathbf{G}_v}{\partial y}\right)dV = 0\end{aligned} \tag{4}$$

As the fish is self-propelled, the water far from the fish body is at rest, i.e. $u = v = 0$ in the inertial frame. The initial condition of computation of fish swimming ($t = 0$), the water in all the field is at rest too. Note that in the context of burst-coast swimming, t/T denotes the time relative to the beginning of the burst-and-coast swimming cycle, which is an enough long time after the beginning of computation.

The density and the dynamic viscosity of water at 20°C are $\rho = 0.998\times10^3$ kg·m^{-3} and $\mu = 1.002\times10^{-3}$ N·s·m^{-2}, therefore for the MT and HT case, Reynolds number in equation (5) are respectively $Re_{L,\,\mathrm{MT}} = L^2\rho/\mu T = 1.92\times10^4$, $Re_{L,\,\mathrm{HT}} = L^2\rho/\mu T = 0.96\times10^4$.

Finite volume method (FVM) is used, to solve the time-dependent N-S equations (4). The details on coupled algorithm of body-fluid interaction, numerical methods and the definitions of power and efficiency can be founded in [7] and [10].

D. Verification and Validation

The CFD platform has been validated and verificated by several cases [7, 10]. More validations are achieved through the whole-body kinematics results, compared with the corresponding experiments, as will be shown in the first part of "RESULTS" section.

III. RESULTS

A. Whole-body kinematics

The computed kinematics of koi carp's whole-body motion is presented in Fig. 4, together with the experimental data. The propulsive velocity, i.e. the transient velocity history of the c.m. is shown in Fig. 5, compared with the experimental data. The propulsive velocity of the fish body in both cases appear the similar typical burst-and-coast manner, that is an accelerating burst stage followed a decelerating coast stage, consistent with the common sense and the records [1].

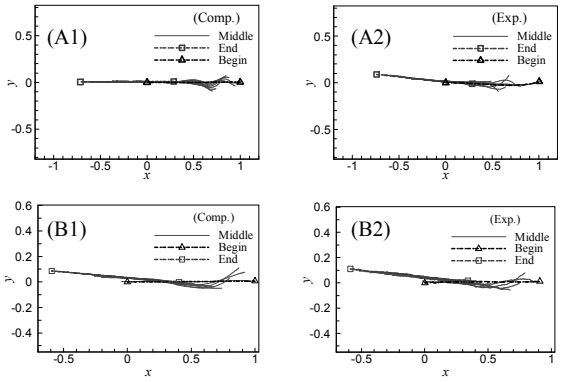

Fig. 4 The predicted whole-body kinematics (presented by the mid-line trajectory) compared with the experimental data in burst-and-coast swimming: (A1) MT, simulation result (A2) MT, experimental data; (B1) HT, simulation result (B2) HT, experimental data ("△" represents the head and end point at the beginning moment, "□" at the last moment.)

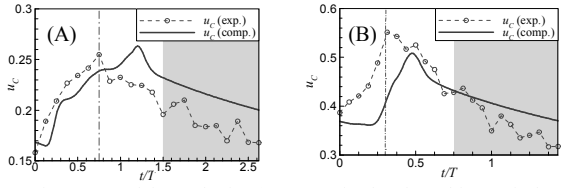

Fig. 5 Propulsive velocity (u_C, magnitude of $\boldsymbol{u}_C$) history in burst-and-coast swimming, the computational result (comp.) and the experimental data (exp.) (A) MT mode and (B) HT mode.

Considering the low resolution (around ten frames per T^*) in the experiments and the degree of approximation of the 2-D fish swimming model, it is reasonable to state that the predicted results agree well with the experiments. Thereby, the results in this section provide validations for our simulation platform.

Meanwhile, the whole-body rotation, namely the turning angle θ_t of the koi carp (in both cases) are predicted, which shows the main kinematic difference between the MT and HT burst-and-coast swimming. In MT burst, the carp accomplish a little negative (clockwise) rotation and a successive positive (counterclockwise) rotation, which lead to its body advancing forward finally. In HT burst, the carp accomplishes a relatively large clockwise rotation (about 6 degrees), that is it turns about 6 degrees to the right. In addition, the carp turns close to the maximum turning angle at the end of the up stroke, which is accordant with previous conclusion [13].

B. Hydrodynamic forces

The transient hydrodynamic forces in the two burst-and-coast swimming modes are given in Fig. 6. It is the hydrodynamic forces that cause the whole-body kinematics revealed in the above section.

In each mode of burst-and-coast swimming, hydrodynamic forces change with time unsteadily and present different characteristics in every stage, different from the periodic state in steady swimming.

Firstly, consider the longitude force C_T. In burst stage, the 'p'-component thrust (C_{T_p}) is much larger than friction drag ($C_{D\_f} = -C_{T\_f}$), so the koi carp accelerate; in the coast stage, both 'p' and 'f' – components are negative, so the koi carp decelerate. Note that the drag in the burst stage $C_{D\_f,\ burst}$ is remarkably larger than that in the coast stage $C_{D\_f,\ coast}$. Above assertions are true not only in MT mode, but also in HT mode. The different points are the wave form and the number of wave crests, which caused by their different undulating kinematics in the two modes.

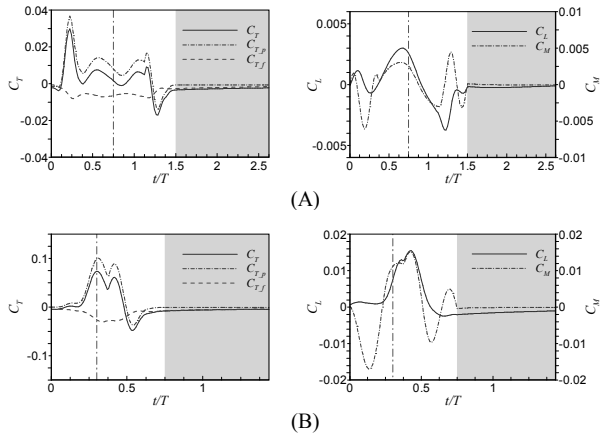

Fig. 6 Hydrodynamic forces in (A) the MT case and (B) the HT case in one cycle.

Secondly, investigate the lateral force C_L. Two modes of burst-and-coast swimming appear essentially different. In the MT mode, because burst 1 and burst 2 are almost antisymmetric, so the lateral force canceled out. In the HT mode, the lateral force is positive (towards the right side of the fish) in all the burst stage, as provides the centrifugal force for its turning motion.

Thirdly, note the moment C_M. The magnitude of the moment in the MT burst is much less than that in HT burst. In the HT burst, up stroke produces a large clockwise moment, and down stroke produces the counterclockwise one. Such two successive moments make the fish body turn an angle. Otherwise in the MT burst, two bursts (one to the right and the other to the left) appear antisymmetric in time, so do the turning motion. Admittedly, in HT burst-and-coast, the fish surely carry out turning motion, and in MT burst-and-coast, fish mainly advance forward.

C. Flow patterns

The hydrodynamics is closely related with the corresponding flow pattern of each mode. With visualization of the simulation results, the flow patterns are shown in Fig. 7 (MT mode) and Fig. 8 (HT mode), where both similarity and difference exist between the two modes. In that MT burst includes two bursts and HT burst includes one burst, the up-stroke and the down-stroke of the tail can be regarded as the fundamental movements in the undulating kinematics. The vortex motion is strongly related to the strokes of the tail.

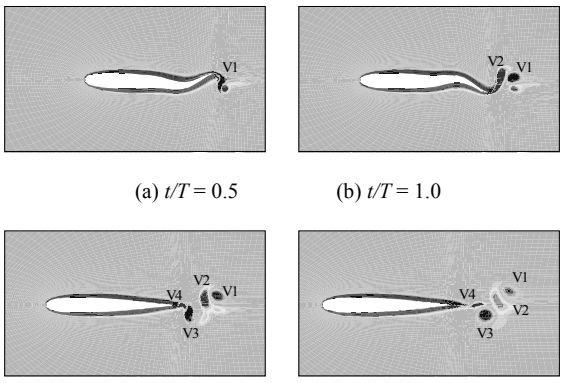

(a) $t/T = 0.5$ (b) $t/T = 1.0$

(c) $t/T = 1.5$ (d) $t/T = 2.0$

Fig. 7 The vortex structure, i.e. vorticity contours in MT burst-and-coast in one cycle.

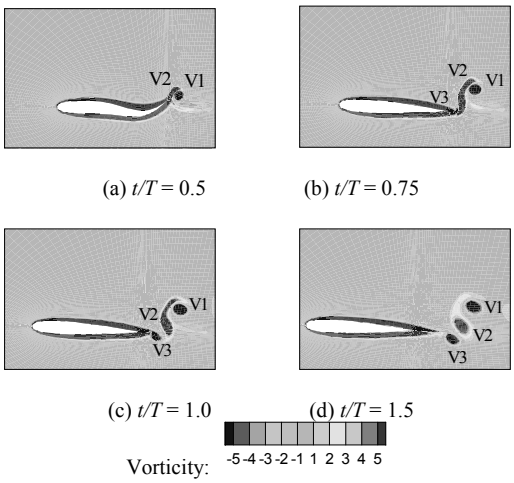

(a) $t/T = 0.5$ (b) $t/T = 0.75$

(c) $t/T = 1.0$ (d) $t/T = 1.5$

Fig. 8 The vortex structure, i.e. vorticity contours in HT burst-and-coast in one cycle.

Firstly in HT burst-and-coast (Fig. 8), the simpler mode, it is clear that the vortex motion is distinctly divided into two stages. In the up stroke stage (Fig. 8a, b), the caudal fin swings to the right, and a pair of

vortices (V1 and V2) forms and sheds laterally to the right from the tail-tip. In the down stroke stage (Fig. 8c, d), the caudal fin back to the middle, another pair of vortices (V2 and V3) forms and sheds backward from the tail-tip. The simulation results of flow pattern confirm the preceding observations in fish turning maneuver [14-17], in that the single-beat turning is essentially the same as HT burst [3, 17].

Secondly in MT burst-and-coast (Fig. 7), the vortex pair consisting of V1 and V2 (Fig. 7a, b) is the similar with that in HT burst-and-coast. The difference includes two points: (1) when the tail swings back to the left (Fig. 7c), the second vortex pair (V2 and V3, same as in HT) sheds to the left, not backward; (2) the third vortex pair (V3 and V4) sheds backward, when the tail withdraws to straight (Fig. 7d), which behaves like the second vortex pair in HT does.

The two kinds of flow pattern show good agreement with experimental results (see Fig. 5 and Fig. 6 in [3]), except that in the experimental data, the last vortex in each mode when the tail draws back to the straight line does not illustrated quite obviously because its small strength.

D. Energetics

As mentioned in the introduction section, researchers concern about whether burst-and-coast is advantageous in energetics, comparing with steady swimming. With the CFD method in this paper, the transient output power of the fish can be computed, definition refers to [10]. Here, the steady flow assumption and the approximate evaluation of energy cost are abandoned, which are unreasonable in most maneuvering situations.

A series of cases of straight line burst-and-coast swimming (in the MT mode) and steady swimming were carried out, where the propulsive velocity in the cases is varied by varying the undulating amplitude. The amplitude, wave length and undulating period are set to be the same between the corresponding cases. The average output power C_P and the propulsive Froude efficiency Fr with the average speed are plotted (Fig. 9), in order to compare the energetic performance of the burst-and-coast swimming and steady swimming. Note that in moderate and low speed ($U \leq 0.32$ in Fig. 9), which covers the range of koi carp swimming in the experiments (where the maximum of the average speed is 1.5 ± 0.6 L·s^{-1}, i.e. 0.24 ± 0.096 nondimensionalized velocity), powers (C_P) of the two are close. In the high speed region ($U \geq 0.32$ in Fig. 9), burst-and-coast swimming costs more energy than steady swimming. In terms of mechanical propulsive efficiency (Fr), burst-and-coast swimming is less efficient than steady swimming.

The result is more convincing than existing estimates because it is the unsteady fluid dynamic equations that are solved. Besides, the conclusion is understandable, as in burst-and-coast swimming the velocity changes more frequently, so more useless work should be done. Although, koi carp still have reasons to use burst-and-coast manner instead of steady swimming, in that burst-and-coast swimming is in deed more free and more maneuverable than the simple steady swimming, as adapted to koi carp's circumstances, such as the inland river, pool or aquarium.

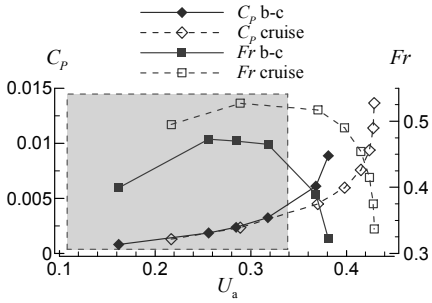

Fig. 9 The energetic quantities average output power C_P and the propulsive Froude efficiency Fr with the average speed U_a, comparing burst-and-coast swimming ('b-c') and steady swimming ('cruise')

IV. DISCUSSION

Main Control mechanisms

The main control mechanisms in burst-and-coast swimming are investigated by comparing the body motion and energetics with the critical factors changed.

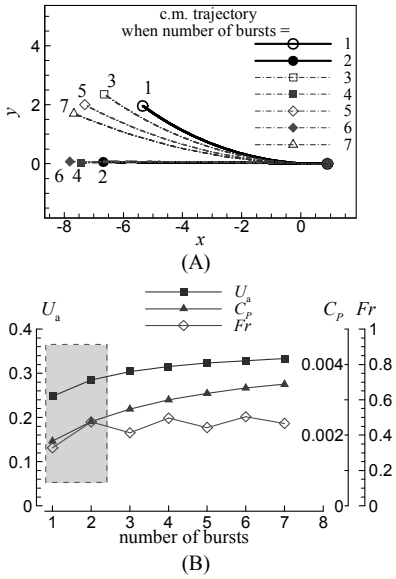

Fig. 10 Effect of number of bursts to the motion and energetics quantities, where all the cases have the same coast time (A) the c.m. trajectories with varied number of bursts in burst-and-coast swimming, (B) the average speed U_a, power C_P and propulsive Froude efficiency Fr with number of bursts changed.

The first control mechanism is how the fish select the number of tail-beat times. The effect of the burst times is shown in Fig. 10, where in Fig. 10A the c.m. trajectories are displayed and in Fig. 10B the energetic parameters are plotted. Note that odd number bursts lead to turning and even number bursts lead to advancing forward, and the largest turning happens when the fish burst only once in the burst stage (HT mode). One time burst and two times bursts are the most optimal on energetics, since with more times the fish

burst, neither the speed nor the efficiency increase obviously, while energy cost increase much more.

So, the fish determines the times of bursts according to whether turning is needed. Statistic data in experiments show that, tuning angle in MT burst-and-coast is 3.0 ± 1.8° and in HT burst-and-coast is 15.3 ± 7.8°, which are both a relatively little value [3]. Statistic data also show that the cases including more than two continuous bursts in the burst stage are rare.

At the second, the average speed is mainly controlled by the undulating amplitude $A_{\max}$. The kinematic and energetic effect of $A_{\max}$ is shown in Fig. 11. Note that as $A_{\max}$ increases, speed increases and energy cost increases more steeply, and efficiency arrives the optimal value in the speed range 0.2~0.3.

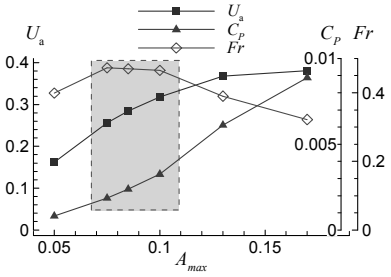

Fig. 11 The Effect of $A_{\max}$ to the average speed U_a, energetic quantities C_P and Fr in koi carp burst-and-coast swimming.

V. CONCLUSIONS

A simulation-based work of a self-propelled fish maneuvering, named burst-and-coast swimming, by solving the full unsteady Navier-Stokes equations and deforming body dynamics equations is presented in this paper. Based on the original experiments, the typical cases of the two basic modes are simulated and their similarities and differences on flow physics are investigated. The computed whole-body kinematic results show good agreement with the experiments. The energetics of burst-and-coast swimming and steady swimming are compared, showing that the former is less efficient than the latter, and the former does not cost less energy than the latter. Several main control mechanisms in burst-and-coast swimming and the issue of friction drag are discussed.

CFD simulation gives more comprehensive kinematic details and flow physics than the living fish experiments, although advancing measurement technologies are fundamental to provide more and more kinematical information. Thus, further collaboration between the two folds will shed new lights on the mechanism study of fish swimming and design of AUV/UUV with high performances.

ACKNOWLEDGEMENTS

This work is supported by the National Natural Science Foundation of China (No. 10332040), the Innovation Project of the Chinese Academy of Sciences (KJCX2-YW-L05) and China Postdoctoral Science Foundation funded project (No. 20080430409).

REFERENCES

[1] J. J. Videler, *Fish Swimming*. London: Chapman & Hall, 1993.

[2] D. Weihs and P. W. Webb, "Optimization of locomotion," in *Fish Biomechanics*, P. W. Webb and D. Weihs, Eds. New York: Praeger, 1983, pp. 339-371.

[3] G. Wu, Y. Yang, and L. Zeng, "Kinematics, hydrodynamics and energetic advantages of burst-and-coast swimming of koi carps (Cyprinus carpio koi)," *J Exp Biol,* vol. 210, pp. 2181-2191, Jun. 2007.

[4] D. Weihs, "Energetic advantages of burst swimming of fish," *Journal of Theoretical Biology,* vol. 48, pp. 215-229, 1974.

[5] J. J. Videler and D. Weihs, "Energetic advantages of burst-and-coast swimming of fish at high speeds," *J Exp Biol,* vol. 97, pp. 169-178, Apr. 1982.

[6] J. Carling, T. L. Williams, and G. Bowtell, "Self-propelled anguilliform swimming: simultaneous solution of the two-dimensional Navier-Stokes equations and Newton's laws of motion," *J Exp Biol,* vol. 201, pp. 3143-3166, Dec. 1998.

[7] Y. Yang, G.-H. Wu, Y.-L. Yu, and B.-G. Tong, "Two-dimensional self-propelled fish motion in medium: an integrated method for deforming body dynamics and unsteady fluid dynamics," *Chinese Physics Letters,* vol. 25, pp. 597-600, Feb. 2008.

[8] S. Kern and P. Koumoutsakos, "Simulations of optimized anguilliform swimming," *J Exp Biol,* vol. 209, pp. 4841-4857, Dec. 2006.

[9] K. S. Yeo, S. J. Ang, X. Y. Wang, and C. Shu, "Simulation of flapping-wing flows and fish swimming/manoeuveres on hybrid meshfree-Cartesian grids by an SVF-GFD method," in *Biological Approaches for Engineering*, University of Southampton, UK, 2008, pp. 22-25.

[10] Y. Yang, G.-H. Wu, Y.-L. Yu, and B.-G. Tong, "Flow Physics of Routine Turns of Koi Carp(Cyprinus Carpio Koi)," *Journal of Biomechanical Science and Engineering,* vol. 4, pp. 67-81, 2009.

[11] H. Liu, R. Wassersug, and K. Kawachi, "A computational fluid dynamics study of tadpole swimming," *J Exp Biol,* vol. 199, pp. 1245-1260, Jun. 1996.

[12] I. Borazjani and F. Sotiropoulos, "Numerical investigation of the hydrodynamics of carangiform swimming in the transitional and inertial flow regimes," *J Exp Biol,* vol. 211, pp. 1541-1558, May. 2008.

[13] D. Weihs, "A hydrodynamical analysis of fish turning manoeuvres," *Proc Roy Soc Lond B,* vol. 182, pp. 59-72, 1972.

[14] J. Jing, X. Yin, and X. Lu, "Hydrodynamic analysis of C-start in Crucian carp," *Journal of Bionics Engineering,* vol. 1, pp. 102-107, 2004.

[15] J. Sakakibara, M. Nakagawa, and M. Yoshida, "Stereo-PIV study of flow around a maneuvering fish," *Experiments in Fluids,* vol. 36, pp. 282-293, 2004.

[16] B. Epps and A. Techet, "Impulse generated during unsteady maneuvering of swimming fish," *Experiments in Fluids,* vol. 43, pp. 691-700, 2007.

[17] G. Wu, Y. Yang, and L. Zeng, "Routine turning maneuvers of koi carp Cyprinus carpio koi: effects of turning rate on kinematics and hydrodynamics," *J Exp Biol,* vol. 210, pp. 4379-4389, Dec. 2007.